Journal of Hazardous Materials 192 (2011) 8–17

Contents lists available at ScienceDirect

Journal of Hazardous Materials

journal homepage: www.elsevier.com/locate/jhazmat

Emulsion polymerization of vinyl acetate: Safe optimization of a hazardous complex process

S. Copelli[a], M. Derudi[a], J. Sempere[b], E. Serra[b], A. Lunghi[c], C. Pasturenzi[c], R. Rota[a,*]

[a] Politecnico di Milano, Dipartimento di Chimica, Materiali e Ingegneria Chimica "G. Natta", via Mancinelli 7, 20131 Milano, Italy
[b] IQS Universitat Ramon Llull, Departament d'Enginyeria Química, Via Augusta 390, 08017 Barcelona, Spain
[c] Stazione Sperimentale per i Combustibili, viale A. De Gasperi 3, 20097 S. Donato M.se, Italy

ARTICLE INFO

Article history:
Received 5 February 2011
Received in revised form 14 April 2011
Accepted 15 April 2011
Available online 22 April 2011

Keywords:
Topological criterion
Vinyl acetate
Safety
Runaway reactions
Optimization

ABSTRACT

Fast and exothermic discontinuous emulsion polymerization processes are particularly difficult to optimize from both safety and productivity point of view because of the occurrence of side undesired reactions (e.g. chain transfer to monomer, backbiting, propagation of tertiary radicals, termination by disproportion, etc.) and the hazards of boiling phenomena and stable foam formation under atmospheric pressure. Moreover, the relevant number of loading, heating and cooling steps, required before starting the monomer addition (that is, the desired reaction), makes a strict product quality reproducibility very difficult to obtain. Under these operating conditions, it is necessary to employ a suitable combined theoretical and experimental procedure able to detect the optimum process dosing time at both the laboratory and the industrial scale. In this work, it is shown how to use the topological criterion theory together with proper adiabatic calorimeter and RC1 experimental data to safely optimize the synthesis of polyvinyl acetate through the radical emulsion polymerization of vinyl acetate by the means of an indirectly cooled isoperibolic semibatch reactor.

1. Introduction

Polymerizations are known to be one of the most frequent causes of thermal runaway (that is, loss of the reactor temperature control occurring whenever the rate of heat removal through the cooling system becomes lower than the rate at which the heat is evolved by the synthesis reactions) in fine chemical industries [1,2] because of three main aspects: (1) the high exothermicity involved [3] (up to 110 [kJ/mol]); (2) the hazard of free radical accumulation that causes sudden propagation reaction rate acceleration (Trommsdorff or gel effect [4,5]); (3) under atmospheric pressure, the occurrence of boiling phenomena followed by stable foam formation above a threshold temperature (in the following referred to as MAT, "Maximum Allowable Temperature" [6]). For all these reasons, a safe optimization of such processes (namely, the search for a dosing time able to maximize both safety and productivity), at both laboratory and industrial scale, is difficult to perform.

Particularly, radical emulsion polymerizations are a class of polymerization reactions that are widespread around the world in order to produce a great variety of homopolymers and copolymers to employ into the production of paints free of flammable, odorous or toxic solvents and easy to use because their high fluidity (emulsions viscosity is independent of the molecular weight of the polymer) [7]. In order to investigate a safe optimization of such processes, polyvinyl acetate (PVA) lattices are an interesting laboratory-scale case-study because the synthesis involves lots of substances loading, heating and cooling steps, a high propagation reaction enthalpy and a strong tendency to accumulate free radicals.

In general, polyvinyl acetate emulsions are milk-white liquids containing 30–55% polymer solids, water, small amounts of emulsifiers, protective colloids and other additives [7]. At the full plant scale, repeatability of emulsion polymerization processes within narrow limits is desirable; this means that the final solids content should be constant within ±1%, the particle size, emulsion viscosity and polymer average molecular mass should vary little from batch to batch and any residual monomer should be maintained within minimum possible narrow limits (<0.5%). In order to achieve these conditions, the formulation of the emulsion polymerization (namely, the recipe) should not be subject to variations such as minor changes of either raw materials or operating conditions [7].

Moreover, other restrictions apply on an emulsion polymerization process in industrial practice. The process should be completed in the shortest possible time; an overall time including loading the chemicals, polymerizing, cooling and unloading should be within 8–12 h to allow working two or three shifts per day. It is desirable to prepare a latex at the highest concentration possible to save time in production, unlike most theoretical work in laboratories

* Corresponding author. Fax: +39 0223993180.
E-mail address: renato.rota@polimi.it (R. Rota).

0304-3894/$ – see front matter © 2011 Elsevier B.V. All rights reserved.
doi:10.1016/j.jhazmat.2011.04.066

Nomenclature

A pre-exponential factor [s^{-1}] or [m^3 s/kmol]; area [m^2]
$C_{diff,pw}$ $= k^{\circ}_{diff,pw} \cdot [N_{mic}]_{w,0} \cdot s_{mic} \cdot t_{dos}$ global constant for the radicals diffusion from polymer particles to water
$C_{diff,wp}$ $= k^{\circ}_{diff,wp} \cdot [I]_{w,0} \cdot s_{mic} \cdot N_A \cdot t_{dos}$ global constant for the radicals diffusion from water to polymer particles
$C_{t,n}$ $= k_{t,w}(T_{rif}) \cdot t_{dos}/(v_{mic} \cdot N_A)$ global constant for the termination reaction in polymer particles
C_{δ} $= k_{p,w}(T_{rif}) \cdot t_{dos} \cdot (\varepsilon_{mp}/(1-\varepsilon_{mp})) \cdot (\rho_M/\rho_P) \cdot (1/N_A) \cdot (1/4\pi v_{mic})$, volume increase constant for a polymer particle
D reactor diameter [m]
D_{diff} diffusion coefficient [m^2/s]
Da_{coal} $= k_{coal} \cdot \sqrt{[I]_{w,0} \cdot V_w \cdot N_A} \cdot [N_{mic}]_{w,0} \cdot V_w \cdot t_{dos}$, Damköhler number for the coalescence of the polymer particles
$Da_{d,w}$ $= f_w \cdot k_{d,w}(T_{rif}) \cdot t_{dos}$, Damköhler number for the thermal decomposition reaction (in water)
$Da_{diff,pw}$ $= k_{diff,pw} \cdot [N_{mic}]^2_{w,0} \cdot 4\pi \cdot r^2_{mic} \cdot t_{dos}/[I]_{w,0} \cdot N_A$, Damköhler number for the radical diffusion from polymer particles to water
$Da_{diff,wp}$ $= k_{diff,wp} \cdot 4\pi \cdot r^2_{mic} \cdot [N_{mic}]_{w,0} \cdot t_{dos}$, Damköhler number for the radical diffusion from water to polymer particles
$Da_{nucl,mic}$ $= 4\pi \cdot D_{diff,wp} \cdot r_{mic} \cdot f_{nucl,mic} \cdot [N_{mic}]_{w,0} \cdot t_{dos}$, Damköhler number for the micellar nucleation
$Da_{nucl,mic,bis}$ $= Da_{nucl,mic} \cdot N_A$, Damköhler number for the micellar nucleation (variation)
$Da_{nucl,omo}$ $= k_{nucl,omo} \cdot k_{p,w}(T_{rif}) \cdot [M]_{w,sat} \cdot t_{dos}$, Damköhler number for the homogeneous nucleation
$Da_{nucl,omo,bis}$ $= k_{nucl,omo} \cdot k_{p,w}(T_{rif}) \cdot [M]_{w,sat} \cdot (([I]_{w,0} \cdot N_A)/[N_{mic}]_{w,0}) \cdot t_{dos}$, Damköhler number for the homogeneous nucleation (variation)
$Da_{p,p}$ $= k_{p,w}(T_{rif}) \cdot [N_{mic}]_{w,0} \cdot t_{dos}/N_A$, Damköhler number for the propagation reaction in the polymeric phase
$Da_{p,w}$ $= k_{p,w}(T_{rif}) \cdot [I]_{w,0} \cdot t_{dos}$, Damköhler number for the propagation reaction in the aqueous phase
$Da_{t,w}$ $= k_{t,w}(T_{rif}) \cdot [I]_{w,0} \cdot t_{dos}$, Damköhler number for the termination reaction in the aqueous phase
E_{att} activation energy [J/kmol]
$f_{nucl,mic}$ micellar nucleation efficiency
f_w initiator thermal decomposition efficiency (in water)
k $= A \cdot \exp(-E_{att}/RT)$, kinetic constant [$s^{-1}$] or [$m^3$ s/kmol]
k_{coal} kinetic constant for the polymer particles coalescence
k_{diff} kinetic constant for the radical diffusion [m/s]
$k_{nucl,omo}$ constant for the homogeneous nucleation
I initiator species
L blade length [m]
M monomer species
m number of monomer units in a radical chain; reacting mass [g] or [kg]
MAT Maximum Allowable Temperature [°C]
N stirrer speed [min^{-1}]
N_{mic} number of micelles
N_p number of polymer particles
n run index; number of monomer units in a radical chain; number of moles [kmol]; number of pseudo-radical species in a polymer particle
P dead polymer chain
$\dot{Q}_{rxn}$ heat power released by the exothermic reaction [W]
QFS quick onset, fair conversion, smooth temperature profile operating conditions
R pseudo-radical species
r particle radius [m]
RW runaway operating conditions
STV starving conditions
T reactor temperature [°C] or [K]
t time [s] or [min]
U overall heat transfer coefficient [W/(m^2 K)]
V/v total volume/single volume [m^3]
Wt $= const \cdot (U \cdot t_{dos}/D)$ Westerterp number

Subscripts and superscripts
amb referred to as environmental conditions
cool referred to as the jacket/coolant
d referred to as the thermal decomposition of the initiator
delay referred to as the delay of the monomer dosing caused by evaporation and successive total condensation
dos referred to as the dosing period
enthalpic referred to as the enthalpic conversion
ext referred to as the external reactor surface
IND referred to as the industrial reactor
LAB referred to as the laboratory reactor
MAX maximum value of a quantity
mic referred to as the micelles
MIN minimum value of a quantity
n referred to as the run index
p referred to as the propagation reaction; referred to as the polymer particles
RCI referred to as the laboratory reactor
rif referred to as the reference temperature (300 [K])
tc referred to as the termination by combination reaction
td referred to as the termination by disproportion reaction
w referred to as the continuous phase (water)
0 referred to as the start of the dosing period
[ ] volume division operator [m^{-3}]

Greek symbols
α experimental parameter taking into account the net power removed by the monomer vaporization and total condensation
γ $= E_{att}/RT_{rif}$, dimensionless activation energy
$\Delta\hat{H}_{rxn}$ reaction enthalpy [cal/g] or [J/kg]
δ_p $= r_p/r_{mic}$, dimensionless polymer particles radius
ε_{mp} $= [M]_{p,sat} \cdot PM_M/\rho_M$, ratio between monomer volume and polymer particle volume when the monomeric phase still exists
ζ_i $= n^{\circ}_i - n_i(t)/n^{\circ}_i$, conversion with respect to the desired species i
$\eta_{p,w}$ $= [N_p]_w/[N_{mic}]_{w,0}$, dimensionless polymer particles concentration (in water)
κ $= \exp(\gamma \cdot (1 - 1/\tau))$, dimensionless kinetic constant
ς correction factor

$\varsigma_{R,w}$	$= [R]_w/[I]_{w,0}$, dimensionless pseudo-radical species concentration (in water)
ξ_{mic}	$= [N_{mic}]_{w,0} - [N_{mic}]_w/[N_{mic}]_{w,0}$, micellar conversion
τ_{cool}^{eff}	$= (R_H\varepsilon \cdot \tau + Wt \cdot (1+\varepsilon) \cdot (1-\omega \cdot \xi_M) \cdot \tau_{cool})/(Wt \cdot (1+\varepsilon) \cdot (1-\omega \cdot \xi_M) + R_H\varepsilon)$, effective coolant temperature
ψ	$= T/T_{cool}$, dimensionless temperature with respect to coolant temperature
ω	experimental factor taking into account the volume contraction when monomer is converted in a dead chain

[7]. The upper limit of the maximum solids content is generally the high viscosity of the latex product, which prevents proper stirring and heat transfer, and the reactor temperature operating mode (e.g. for isoperibolic processes a lower solids content, usually 30–35%, is preferred).

In this work, the topological criterion theory [8,9] has been used to safely optimize the free radical emulsion homopolymerization of vinyl acetate (VA) thermally initiated by potassium persulphate (KPS). Particularly, an indirectly cooled semibatch reactor (RC1, 1 L, Mettler Toledo) operated in the isoperibolic control mode (which is simpler to realize in an industrial plant than the isothermal one) has been chosen for the laboratory experiments. Finally, the scaled-up operating conditions have been identified using two different procedures: the first one is based on the mathematical model developed and validated at the laboratory-scale and the second one is based on order-of-magnitude considerations.

2. Optimization–scale-up procedure

The topological criterion theory [8,9] states that, for a semibatch process carried out under the isoperibolic control mode, the boundary between runaway and "Quick onset, Fair conversion, Smooth temperature profile" conditions with respect to a desired product (QFS [10,11]) is identified by an inversion of the topological curve showing a concavity towards right. Particularly, this curve shows all the possible thermal behavior regions of an isoperibolic SBR obtainable by varying one system constitutive parameter (in the polymerization case, the dosing time) in a suitable range. If the dosing time is the topological curve generating parameter, the following thermal behavior regions can be encountered: runaway (RW, sharp temperature profile characterized by high maximum temperature increase with respect to the initial reactor temperature and sudden conversion variations either after or before the end of the dosing period), QFS (smooth temperature profile characterized by medium maximum temperature increase with respect to the initial reactor temperature and almost linear conversion variations during the dosing period that implies high reactor productivity) and STARVING (STV, squared temperature profile characterized by low maximum temperature increase with respect to the initial reactor temperature and a forced linear conversion during the dosing period that implies low reactor productivity). The topological curve can be drawn by solving the mathematical model that describes the analyzed system for each investigated value of the generating parameter and, then, reporting onto a bidimensional diagram the obtained reactor temperature maxima divided by the coolant temperature, $\psi_{MAX,theo} = T_{MAX,theo}/T_{cool}$, and the conversion with respect to the desired product in correspondence of such maxima, $\zeta(\psi_{MAX,theo})$. In the presence of only one exothermic reaction (in the polymerization cases, the propagation reaction), such a curve can be generated also experimentally by measuring, through a set of isoperibolic tests carried out in a laboratory calorimeter, the maximum reactor temperature, $T_{MAX,\mathrm{exp}}$, and the enthalpic conversion in correspondence of such a maximum, $\zeta_{enthalpic,MAX} = \int_0^{t_{MAX}} \dot{Q}_{rxn}(t)dt/(\Delta\hat{H}_{rxn} \cdot m)$.

A suitable combination of these two approaches can be employed to develop an integrated theoretical–experimental procedure able to safely optimize and scale-up whatever complex reacting system where only a single exothermic reaction is predicted to occur and laboratory experiments must be complemented by a reliable mathematical model.

This is the case of the emulsion polymerization of vinyl acetate, where the desired product is the homopolymer (PVA) and the most important operating parameter to optimize and scale-up the process is the monomer dosing time, t_{dos}. Particularly t_{dos}, at both laboratory and industrial scale, should be minimum to obtain the maximum productivity of PVA fulfilling the safety constraints experimentally determined.

The combined theoretical–experimental optimization–scale-up procedure discussed in this work is summarized in Fig. 1 and it involves a minimum of six steps.

1. Reactor typology, temperature control mode, cooling system characteristics and operational list (namely, recipe) have to be selected for the laboratory experiments.
2. Calorimetric screening tests must be carried out in order to characterize the thermal behavior of reactants, products, and reacting mixture in a suitable temperature range.

At first, differential scanning calorimetry (DSC) experiments must be performed for both reactants and products to detect if any thermal decomposition or oxidation can be triggered in the selected temperature range (e.g. −10 to 280 °C).

Then, a set of isoperibolic syntheses at different monomer dosing times has to be carried out to detect the minimum temperature in correspondence of which the reacting mixture under atmospheric pressure starts to boil vigorously forming foams. Such a temperature varies with the monomer feeding rate, the degree of reaction conversion and the thermodynamic properties of the reacting mixture; therefore, at least three different isoperibolic syntheses at a 50 ml scale (batch and two different dosing times) must be planned. It must be stated that boiling and foaming of the reaction mixture may also be avoided by operating the reactor under its autogeneous pressure. This is common for industrial emulsion polymerizations.

3. Reaction rate expressions (usually in a power law form) must be determined by the means of either one isoperibolic or one adiabatic temperature vs. time data fitting.

This test is usually carried out in an isoperibolic RC1 (the first commercialized reaction calorimeter issued by Mettler Co.) like laboratory reactor (runaway and starving conditions must be obviously avoided). However, if the isoperibolic test does not cover the full temperature range of interest, either PHI-TEC II or ARC adiabatic tests can be used for kinetic parameters fitting. Moreover, if the adiabatic temperature rise associated to the exothermic reaction is below the previously determined MAT constraint, a RC1 batch adiabatic test can be used instead of the isoperibolic one. This allows for investigating the entire range of normal and upset operating temperatures but can be dangerous due to the batch-like conditions.

4. Combined theoretical and experimental construction of the topological curve in order to determine the runaway–QFS transition and the optimum dosing time at the laboratory-scale.

First of all, starting from a minimum dosing time value, $t_{dos,MIN}$, a sequence of numerical simulations using different dosing time

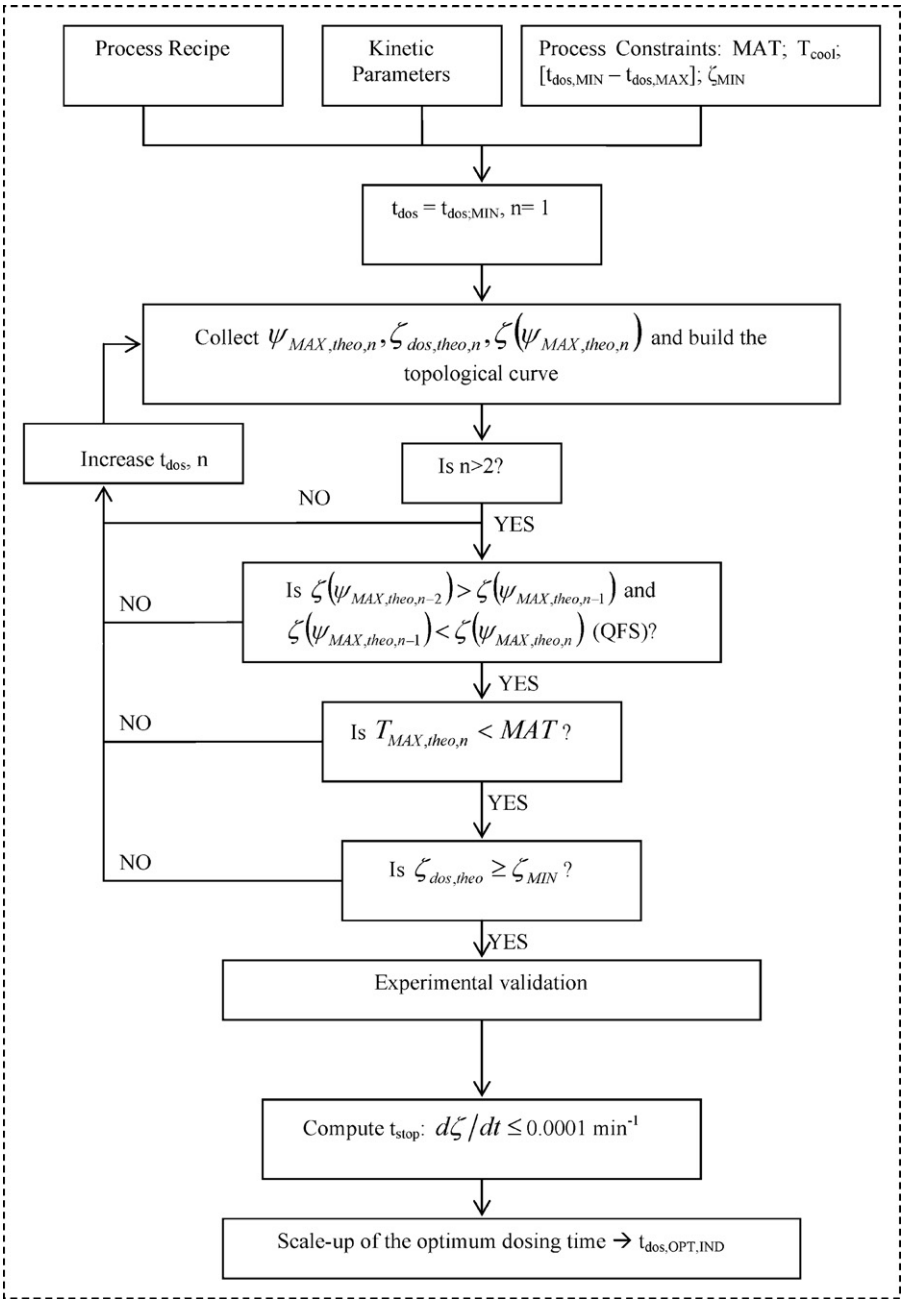

Fig. 1. Scheme of the integrated theoretical–experimental optimization–scale-up procedure.

values must be carried out to generate the topological curve. Particularly, the ratio of the theoretical maximum reactor temperature to the coolant temperature, $\psi_{MAX,theo} = T_{MAX,theo}/T_{cool}$, the conversion with respect to the polymer species in correspondence of such a maximum, $\zeta(\psi_{MAX,theo})$, and the end of the dosing period, $\zeta_{dos,theo}$, must be computed and all $(\zeta(\psi_{MAX,theo}), \psi_{MAX,theo})$ couples must be reported onto the plane where the topological curve is located. When a concavity of the topological curve towards right is detected, this means that the runaway–QFS transition boundary has been found.

To verify if these conditions can be safely used, the following constraints must be checked:

$$T_{MAX,theo,n} < \text{MAT} \quad (1)$$

$$\zeta_{dos,theo,n} \geq \zeta_{MIN} \quad (2)$$

where n is the index of the nth dosing time investigated, MAT is the aforementioned Maximum Allowable Temperature for the considered system and ζ_{MIN} is the minimum conversion required at the end of the dosing time, according to productivity constraints.

If check (1) and (2) are fulfilled the optimum laboratory dosing time ($t_{dos,OPT,LAB}$) has been found. If not the construction of the topological curve must continue (increasing t_{dos}) until they are fulfilled.

Once a suitable value for t_{dos} is identified, in order to validate the procedure, a few isoperibolic RC1 tests at different dosing times (one of them at $t_{dos,OPT,LAB}$) must be carried out and each run has to be classified into one of the following thermal behavior classes: runaway, QFS and STARVING. Moreover, for each experiment, maximum reactor temperature ($T_{MAX,exp}$) and calorimetric conversion corresponding to such a maximum ($\zeta_{MAX,cal}$) must be measured and reported onto the reduced phase portrait where the theoretical topological curve has been generated. If a good agreement between

model predictions and experimental results is obtained, the dosing time calculated from the theoretical topological curve can be considered as the optimum one.

5. Once the optimum dosing time has been established at the laboratory-scale, the time at which the process can be stopped must be identified. Theoretically, such a time corresponds to theoretical conversion variations lower than 0.0001 min^{-1}, that is, when the production rate can be considered negligible. From a practical point of view, in these conditions the process does not make sense. Obviously, the real stop time will be lower than this value and it might be determined by a cost/benefit analysis.
6. Finally, the optimum laboratory dosing time must be scaled-up to the industrial conditions. This can be achieved through two different methods.

The first one is based on the assumption that the kinetics determined at the laboratory-scale holds true also at the industrial one. In this case, the theoretical part of the optimization procedure presented in step 4 can be applied to determine the optimal industrial dosing time by inserting into the mathematical model the industrial reactor characteristics.

The second one is based on an order-of-magnitude procedure which requires that the cooling efficiencies at both the laboratory and the full plant scale being equal. These cooling efficiencies may be represented by a dimensionless number called cooling [10–14] or Westerterp number [15], which represents the ratio between the characteristic time at which the heat evolved by the reaction is accumulated into the system and the characteristic time at which this heat is removed by the cooling system. Referring to the laboratory and the industrial scale, such numbers may be expressed by the following equations:

$$Wt_{LAB} = const \cdot \left(\frac{U_{LAB} \cdot t_{dos,LAB}}{D_{LAB}} \right) \quad (3)$$

$$Wt_{IND} = const \cdot \left(\frac{U_{IND} \cdot t_{dos,IND}}{D_{IND}} \right) \quad (4)$$

If $Wt_{LAB} = Wt_{IND}$, the ratio of industrial to laboratory dosing time is roughly proportional to the product of two factors:

$$\frac{t_{dos,IND}}{t_{dos,LAB}} = \frac{D_{IND}}{D_{LAB}} \cdot \frac{U_{LAB}}{U_{IND}} \quad (5)$$

The first one (which is the ratio of industrial to laboratory reaction vessel characteristic dimensions) is always much higher than 1 and, mostly, implies a dosing time increase when moving from laboratory to industrial scale. The second one (which is the ratio of laboratory to industrial effective overall heat transfer coefficients) decreases as industrial reactor cooling efficiency increases: such a behavior is logical, since a high reactor cooling efficiency allows for a lower dosing time. This factor can be estimated through standard correlation [16] such as (for propeller stirrers) $U_{LAB}/U_{IND} = (L_{LAB}/L_{IND})^{1/3} \cdot (N_{LAB}/N_{IND})$, with L and N being the blade width and the stirrer speed, respectively. Therefore, once dimensions and cooling system characteristics of the industrial reactor have been defined, the optimum scaled dosing time can be obtained from the laboratory one by the means of Eq. (5).

The two approaches can be also used together and their results compared for the sake of cross-validation.

3. Results

As a case-study the emulsion polymerization of vinyl acetate has been investigated experimentally to assess the practical feasibility of the proposed procedure.

Table 1
Process recipe and reactor characteristics for the free radical emulsion homopolymerization of vinyl acetate thermally initiated by KPS.

Initial load and dosed stream	Cooling system
279 g water	Jacket: external (T_{jacket} = 75 °C)
2.5 g SLS	Coolant: silicon oil
0.5 g Na_2CO_3	Nominal volume: 1 [L]
1.0 g KPS	UA_0 = 2.44 [W/K]
130 g vinyl acetate	

3.1. Experimental setup

In order to perform a polyvinyl acetate laboratory synthesis as close as possible to that one carried out at industrial scale, a RC1 equipment (MP06, 1 L, Mettler Toledo), indirectly cooled by means of an external jacket, has been used with the following operational list: (1) distilled water (W, continuous medium), sodium lauryl sulphate (SLS, surfactant) and sodium carbonate (Na_2CO_3, buffer) are loaded into the reactor and, then, heated up to 80 °C in 40 min activating an isothermal control mode; (2) to allow for the formation of SLS micelles (that will contain the growing polymer chains), the mixture is kept at 80 °C for 1 h; (3) potassium persulphate (KPS) is loaded one-shot into the reactor and, then, the temperature control mode is shifted to isoperibolic (T_{cool} = 75 °C) providing a waiting time of 15 min to allow for the reactor and jacket temperatures equilibration; (4) vinyl acetate is dosed through a pump. Reactants and reactor characteristics are summarized in Table 1.

3.2. Calorimetric screening tests

In order to characterize the thermal behavior of the substances that will be involved into the process and detect the system MAT parameter, differential scanning calorimetry (DSC) tests and a set of 50 ml scale syntheses at different monomer dosing times have been carried out.

Particularly, dynamic DSC tests have been performed on potassium persulphate, sodium lauryl sulphate and polyvinyl acetate (see Fig. 2), while an isothermal DSC test has been carried out on vinyl acetate (Fig. 3) using a Mettler Toledo DSC 823^e apparatus and stainless steel, medium pressure viton/120 μL crucibles. All DSC tests have been performed under nitrogen atmosphere to avoid eventually oxygen contributions.

For what concern potassium persulphate, whose DSC test has been reported in Fig. 2A, an exothermic effect in correspondence of 188 °C has been detected. Such a phenomenon can be ascribed to the thermal decomposition of the crystalline solid.

On the contrary, as shown in Fig. 2B, two endothermic effects (the former at about 47 °C, the latter at about 92 °C) have been evidenced for sodium lauryl sulphate. Such phenomena correspond to a solid phase transition between two different crystalline phases and a melting, respectively.

For polyvinyl acetate, as shown in Fig. 2C, only one endothermic effect (at about 28 °C) has been observed in the investigated temperature range (−10 to 190 °C) corresponding to a glass transition.

Finally, for vinyl acetate it can be observed from the isothermal DSC test reported in Fig. 3 that no self-initiated polymerization reactions occur at the selected temperature (75 °C) after more than 300 min.

For what concern the MAT determination, a set of three isoperibolic 50 ml scale tests at different monomer feeding rate has been carried out. Particularly, a 100 ml flask (supplied with a thermocouple connected with an automatic temperature data recorder and a magnetic stirrer) has been inserted into a thermostatic water bath, whose temperature has been maintained at 75 °C (in order to realize the isoperibolic mode), and loaded with 32.3 g of a water/SLS emulsion previously prepared. When water bath and flask ther-

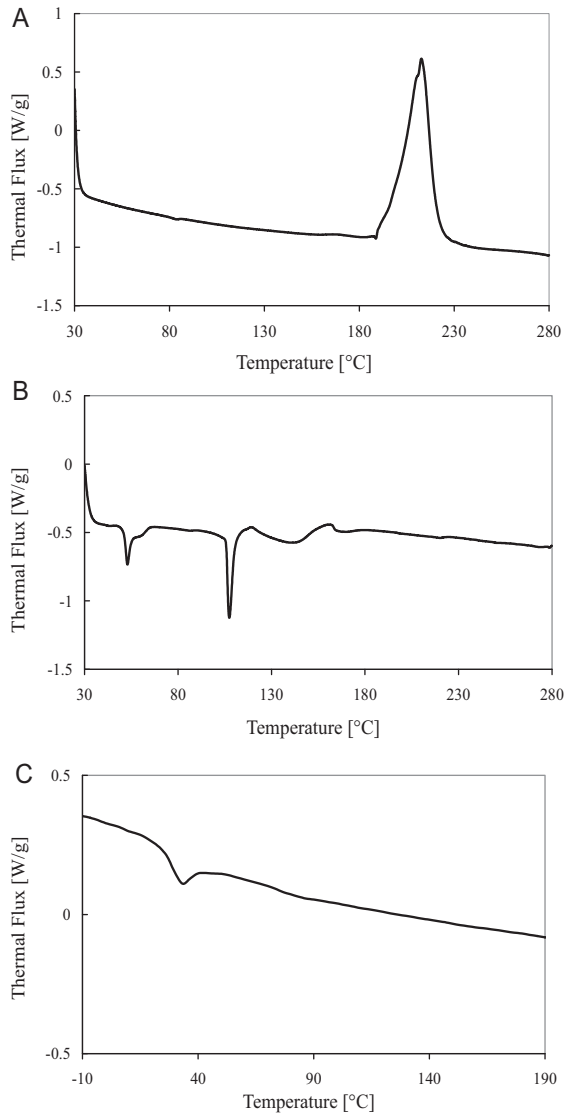

Fig. 2. Dynamic DSC thermal characterization in nitrogen atmosphere: (A) potassium persulphate (KPS), sample amount, 4.20 mg; heating rate, 5 °C/min; investigated temperature range, 30–280 °C. (B) Sodium lauryl sulphate (SLS), sample amount, 4.50 mg; heating rate, 5 °C/min; investigated temperature range, 30–280 °C. (C) Polyvinyl acetate (PVA, MW = 194,800), sample amount, 4.94 mg; heating rate, 5 °C/min; investigated temperature range, −10 to 190 °C.

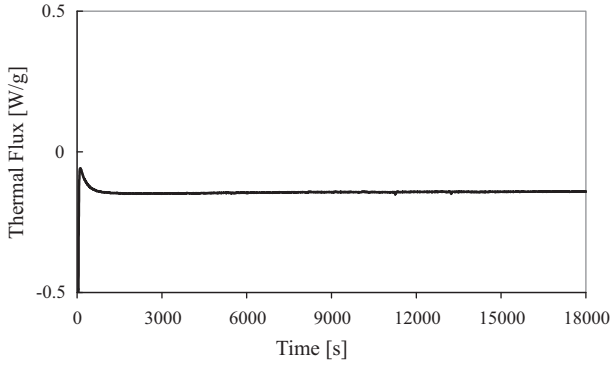

Fig. 3. Isothermal DSC characterization of vinyl acetate (VA) in nitrogen atmosphere: sample amount, 1.08 mg; investigated temperature: 75 °C. The initial spike is not significant because it represents a thermal adjustment of the DSC apparatus signal (sample crucible insertion).

Table 2
Process recipe, dosing times and reacting mixture boiling temperatures for the investigated 50 ml scale vinyl acetate emulsion homopolymerization synthesis.

Recipe	
32 g	Water
0.3 g	SLS
0.06 g	Na_2CO_3
0.1 g	KPS
15 g	Vinyl acetate
Set of 50 ml scale synthesis	

Run	t_{dos} [min]	$T_{boiling}$ [°C]
1	0	83
2	5	No boiling
3	10	No boiling

mocouple equilibrium has been reached, two different operations must be performed according to the reactor operational mode: batch or semibatch. For a semibatch synthesis, KPS is loaded one shot and immediately after the monomer feeding is started. On the contrary, for a batch synthesis, all monomer is loaded into the flask and a new thermocouple equilibration is waited. Then KPS is loaded one shot.

Table 2 lists the recipe followed for each synthesis, all the monomer dosing times used and the temperature at which a boiling phenomenon has been observed.

As it can be noticed from Table 2, the minimum temperature at which the reacting mixture starts to boil vigorously is 83 °C (run 1). Such a temperature can be considered, as a first approximation, as the MAT parameter.

3.3. Kinetic determination

Since the adiabatic temperature rise for this VA emulsion polymerization is equal to 82 °C, it is not possible to perform an adiabatic RC1 test to determine the reaction kinetics because boiling phenomena would start before the reaction completion. Therefore, an isoperibolic RC1 experiment with a dosing time equal to 10 min has been carried out. This guarantees that the process is performed under neither dangerous runaway nor starved operating conditions. Using this RC1 test and the mathematical model reported in Appendix A, a data fitting of the constitutive model parameters summarized in Table 3 has been performed. In Fig. 4, experimental and simulated temperature vs. time profiles are compared, show-

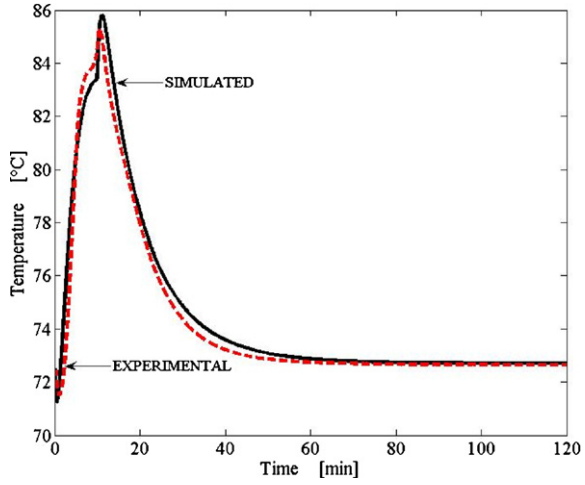

Fig. 4. Experimental (dashed line) and simulated (continuous line) temperature vs. time profiles for the isoperibolic RC1 test used to fit the constitutive model parameters.

Table 3
Constitutive model and kinetic parameters for the free radical emulsion homopolymerization of vinyl acetate thermally initiated by KPS. In the last column, "This work" means that the value has been estimated fitting the isoperibolic RC1 curve reported in Fig. 4.

A_d	1/s	5.33×10^{15}	This work
E_d	kJ/kmol	1.23×10^{5}	This work
f_w	–	0.35	This work
A_p	m^3/(kmol s)	1.4791×10^{7}	This work
E_p	kJ/kmol	2.066×10^{4}	This work
A_t	m^3/(kmol s)	3.70×10^{9}	[21]
E_t	kJ/kmol	1.33×10^{4}	[21]
$k_{nucl,omo}$	–	3.01×10^{-3}	[20]
$f_{nucl,mic}$	–	1.00×10^{-5}	[20]
k_{coal}	m^3/s	2.80×10^{-28}	This work
$D_{diff,wp}$	m^2/s	3.91×10^{-10}	This work
$D_{diff,pw}$	m^2/s	3.10×10^{-10}	This work
ΔH_{rxn}	kJ/mol	89.1	[21]
ε	–	0.48	This work
R_H	–	0.48	This work
$(UA)_{ext}$	–	3.75×10^{-4}	This work
t_{delay}	s	8	This work
α	–	2.98×10^{-4}	This work
ς	–	0.2	This work
ω	–	−1.15	This work
r_{mic}	m	2.50×10^{-9}	[20]
$[E]_{w,sat}$	kmol/m^3	2.43×10^{-9}	[20]
$[M]_{w,sat}$	kmol/m^3	0.2398	[20]
$[M]_{p,sat}$	kmol/m^3	6.510	[20]
PM_M	kg/kmol	86.09	–

ing a good agreement among RC1 experimental data and numerical predictions.

3.4. Combined theoretical–experimental optimization

Using model parameters summarized in Table 3, it is possible to draw the theoretical topological curve by solving Eq. (A.1) for different dosing times (starting from $t_{dos,MIN}$ = 7.5 min to $t_{dos,MAX}$ = 30 min, t_{dos} step being equal to 30 s). Fig. 5 shows the obtained topological curve. Particularly, it is possible to observe the transition inversion (labeled as point A), at which the system thermal loss of control shifts its occurrence from times lower than the dosing period to times higher, followed by the QFS inversion (labeled as point B), in correspondence of which there is a transition between runaway and high productive dosing time control conditions, and the starving inversion (labeled as point C), in correspondence of which there

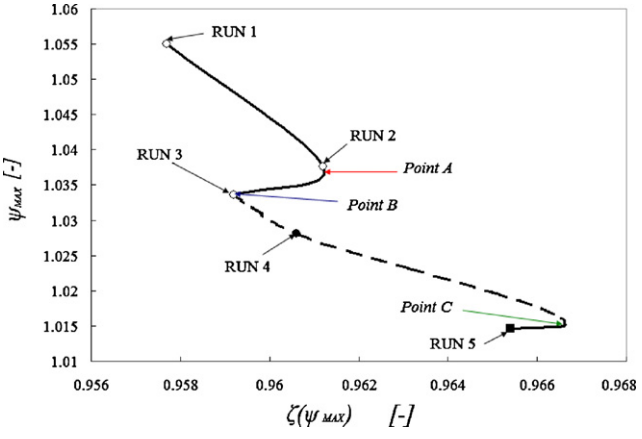

Fig. 5. Theoretical topological curve for the free radical emulsion homopolymerization of vinyl acetate thermally initiated by KPS. T_{cool} = 75 °C, t_{dos} [5–30] min and model parameters as in Table 3. Experimental runs are compared with the corresponding theoretical ones by means of arrows. (○) Runaway run, (●) QFS run, (■) starving run (—) runaway region, (- -) QFS region, and (- . -) starving region. A represents the transition inversion, B the QFS inversion and C the starving inversion.

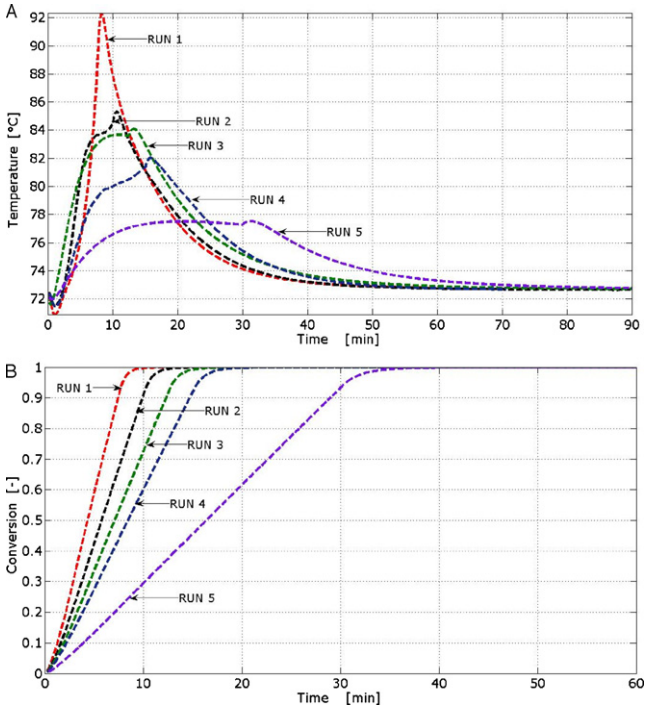

Fig. 6. Experimental temperature (A) and calorimetric conversion (B) vs. time profiles for the free radical emulsion homopolymerization of vinyl acetate thermally initiated by KPS (see Tables 3 and 4).

is a transition between high productive dosing time control conditions and low productive dosing time control conditions.

Then, the optimum dosing time is iteratively searched for by checking constraints (1) and (2) from the dosing time at which the QFS inversion occurs, $t_{dos,QFS}$ (point B in Fig. 5) to that one at which the starving inversion occurs, $t_{dos,STV}$ (point C in Fig. 5). For the analyzed system, the theoretical QFS boundary is detected for a dosing time equal to 12.5 min. In correspondence of this point, a local minimum (since it is referred to the investigated dosing time range) of the conversion with respect to the desired polymer species has been observed. The minimum dosing time able to satisfy constraints (1) and (2) is equal to 15 min (run 4). This dosing time can be considered optimized from both safety ($T_{MAX,theo}$ = 82.2 °C is lower than the MAT = 83 °C) and productivity point of view ($\zeta_{dos,theo}$ = 0.9195 is larger than the minimum desired conversion at the end of the dosing period, ζ_{MIN} = 0.90).

Both the theoretical topological curve and the optimum dosing time must be validated through a set of isoperibolic RC1 runs, whose dosing times have to cover the whole range used to generate the theoretical topological curve. In this work, five isoperibolic experiments, summarized in Table 4, have been carried out.

The corresponding experimental temperature and calorimetric conversion vs. time profiles are shown in Fig. 6, while Table 4 also reports, for each experiment, the maximum reactor temperature ($T_{MAX,exp}$) and the calorimetric conversion corresponding to such a maximum ($\zeta_{MAX,cal}$) and at the end of the dosing period ($\zeta_{dos,exp}$). Moreover, the same table also compares the theoretical and experimental classification of each run in terms of thermal behavior (RW, QFS or STV). Each ($T_{MAX,exp}$, $\zeta_{MAX,cal}$) couple has been located onto the diagram reported in Fig. 5. From both Fig. 5 and Table 4, it is possible to highlight that the boundary between RW and QFS thermal behavior is the same from both model and experimental analysis. This cross-validation strongly supports the reliability of the obtained results.

Finally, for the sake of completeness, latex properties for each experimental run have been measured to verify that a product

Table 4
Theoretical and experimental results comparison for the free radical emulsion homopolymerization of vinyl acetate thermally initiated by KPS. The consequences of each run have been reported by specifying the level of risk experienced at the RC1 scale for the various operating conditions.

Run	t_{dos} [min]	$T_{MAX,exp}$ [°C]	$\zeta_{MAX,cal}$	$\zeta_{dos,exp}$	Experimental classification	Theoretical classification	Consequences
1	7.5	92.28	0.956	0.905	RW	RW	High risk Strong boiling and foam formation
2	10	85.32	0.960	0.907	RW	RW	Medium risk Moderate boiling and foam
3	12.5	84.13	0.955	0.915	QFS	RW/QFS	Low risk Low boiling—No foam
4	15	82.02	0.960	0.920	QFS	QFS	Low risk Low boiling—No foam
5	30	77.54	0.963	0.934	STV	STV	Extremely low risk No boiling—No foam

Table 5
Global solids content, viscosity, pH, residual monomer and particle size results for each experimental run performed (see Table 4). Theoretical residual monomer and final particles size results have been also reported.

Run	t_{dos} [min]	Solids content [%]	Viscosity [cP]	pH	Residual monomer [%]		Mean particles size [nm]		Physical Properties
					Exp	Theo	Exp	Theo	
1	7.5	33.8	6.88-7.04	3.75	<0.1	<0.01	138	126	Acceptable
2	10	33.6	6.56-6.88	4.45	<0.1	<0.01	156	148	Acceptable
3	12.5	34.7	7.52-7.68	4.23	<0.1	<0.01	159	160	Acceptable
4	15	34.5	7.20-7.36	4.34	<0.1	<0.01	162	165	Acceptable
5	30	34.8	6.88-7.04	4.71	<0.1	<0.01	171	185	Acceptable

quality close to the one required by industrial standards has been achieved in the laboratory tests. Particularly, global solids content, viscosity, pH, residual monomer and particle size results have been collected and reported in Table 5 and, where possible, compared with the theoretical results obtained from the numerical simulations.

Such analysis has been performed according to standard quality analysis procedures [17,18] and, as it can be seen from Table 5, a good agreement between experimental results and theoretical predictions has been achieved. Particularly, for what concern particles size and particles size distribution of run 4 (optimal operating conditions), an image obtained from a scanning electron microscope (SEM) has been reported in Fig. 7. It can be noticed that the mean particles size is about 180 nm and all particles show, more or less, the same dimensions. This agrees with the results reported in Table 5 which have been obtained by means of Rayleigh scattering measures.

3.5. Stop time determination

The time at which the batch period can be terminated is referred to as stop time and it corresponds to a theoretical conversion variation lower than 0.0001 min^{-1}. In this case, it has been found to be equal to 30 min. The real stop time will be lower than this value and it can be determined by a cost/benefit analysis.

Table 6
Process recipe and industrial reactor cooling system for the free radical emulsion homopolymerization of vinyl acetate thermally initiated by KPS.

Initial load and dosed stream	Cooling system
2790 kg Water 25 kg SLS 5 kg Na_2CO_3 10 kg KPS	Jacket: external (T_{jacket} = 75 °C) Coolant: water/steam Nominal volume: 6 m^3 UA_0 = 5000 [W/K]
1300 kg Vinyl Acetate	Stirring speed: 30 rpm Blade length: 0.75 m

3.6. Optimum dosing time scale-up

Finally, the two methods reported in step 6 of Section 2 can be applied to scale-up the optimum laboratory dosing time.

Using the industrial reactor parameters reported in Table 6 (for which experimental data are not available at the moment), the

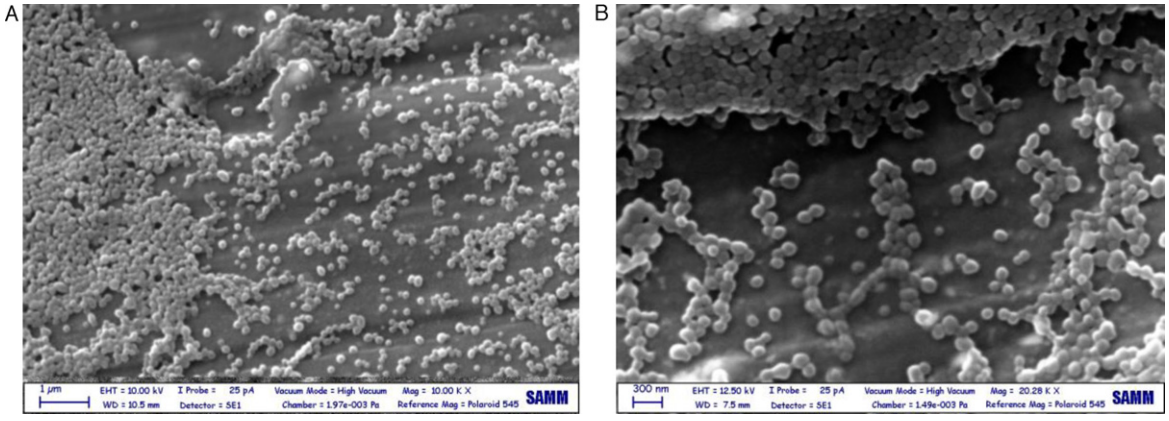

Fig. 7. SEM images at two different resolutions (1 μm (A) and 300 nm (B)) for the final PVA latex obtained in run 4 (see Table 4).

first approach provides an optimum industrial dosing time equal to 100 min, while the second one a value equal to 120 min. As it can be noticed, such values are quite close each other thus cross-confirming the reliability of the suggested methodologies.

4. Conclusions

In this work it has been shown that the topological criterion theory is useful to develop a combined theoretical–experimental procedure able to both optimize and scale-up a complex hazardous reacting system where only one exothermic reaction occurs. Using as case-study the radical emulsion homopolymerization of vinyl acetate thermally initiated by potassium persulphate, a good agreement between theoretical predictions (namely, the shape of the topological curve and its thermal behavior regions) and experimental results (RC1 runs) has been achieved. Particularly, it has been proven that the transition, QFS and starving inversions represent real thermal behavior boundaries that can be experimentally identified. It is important to stress that the principle of safe operation for whatever reacting system should always contain the physical/chemical properties of chemicals used, plant and process design and thermokinetics within the system. Credible worst case scenarios which may be encountered in reactor must be verified by adiabatic calorimetry, including any possible upset/fault conditions. Besides, the data detected in adiabatic calorimeter are the essential parameters for the safe emergency relief system design in an acceptable risk. Therefore, RC1 runs should always be complemented by adiabatic calorimetry tests to assure the maximum temperature and pressure that can be sustained in the standard design of a reactor system.

Acknowledgements

The authors wish to express their gratitude to Prof. G. Storti for his precious suggestions about emulsion polymerizations theory, and to S. Martínez Pié, D.P. Karunaratnage Wattegama, L. Gigante, M. Dellavedova and P. Cardillo for a part of the laboratory experimentations. Moreover, financial support of the Italian MIUR – PRIN2007 is gratefully acknowledged.

Appendix A. Mathematical model

The following kinetic scheme shows the main reactions that are involved into the PVA synthesis:

1. Initiation $I \xrightarrow{k_d} 2R$
2. Propagation $R + M \xrightarrow{k_p} R$
3. Chain transfer to monomer $R + M \xrightarrow{k_{fm}} R + P$
4. Termination by combination $R + R \xrightarrow{k_{tc}} P$
5. Termination by disproportion $R + R \xrightarrow{k_{td}} 2P$

where I represents the initiator species (in this case, KPS), $R = \sum_{n=1}^{\infty} R_n$ is a pseudo-radical which represents all radical species independently of their chain length ("Terminal Kinetic Model", TMK [19]), M is the monomer (in this case, VA) and P represents the dead polymer chain (neither branching nor molecular weight distribution analysis have been considered according to the TMK theory).

The reactive step (dosing and polymerization) can be modeled by the means of the following system of algebraic – differential equations expressing mass and energy balances.

$$
\begin{cases}
\dfrac{d\zeta_I}{d\vartheta} = Da_{d,w} \cdot \kappa_{d,w}(\tau) \cdot (1 - \zeta_I) \\
\dfrac{d\varsigma_{R,w}}{d\vartheta} = 2 \cdot Da_{d,w} \cdot \kappa_{d,w}(\tau) \cdot (1 - \zeta_I) - 2 \cdot Da_{t,w} \cdot \kappa_{t,w}(\tau) \cdot {\varsigma_{R,w}}^2 - Da_{diff,wp} \cdot \delta_p \cdot \varsigma_{R,w} \cdot \eta_{p,w} \\
-Da_{nucl,mic,bis} \cdot \varsigma_{R,w} \cdot (1 - \xi_{mic}) - Da_{nucl,omo} \cdot \kappa_{p,w}(\tau) \cdot \varsigma_{R,w} + Da_{diff,pw} \cdot \delta_p \cdot {\eta_{R,w}}^2 \cdot n \\
\dfrac{d\zeta}{d\vartheta} = Da_{p,w} \cdot \kappa_{p,w}(\tau) \cdot \left(\dfrac{\vartheta}{1 + \vartheta_{delay}} - \zeta \right) \cdot \varsigma_{R,w} + Da_{p,p} \cdot \kappa_{p,w}(\tau) \cdot \left(\dfrac{\vartheta}{1 + \vartheta_{delay}} - \zeta \right) \cdot n \cdot \eta_{p,w} \\
\dfrac{dn}{d\vartheta} = -C_{t,n} \cdot \kappa_{t,w}(\tau) \cdot \dfrac{n \cdot (n-1)}{\delta_p^3} + C_{diff,wp} \cdot \delta_p \cdot \varsigma_{R,w} - C_{diff,pw} \cdot \delta_p \cdot \eta_{p,w} \cdot n \\
\dfrac{d\eta_{p,w}}{d\vartheta} = Da_{nucl,mic} \cdot \varsigma_{R,w} \cdot (1 - \xi_{mic}) + Da_{nucl,omo,bis} \cdot \kappa_{p,w}(\tau) \cdot \varsigma_{R,w} - Da_{coal} \cdot {\eta_{p,w}}^2 \cdot \sqrt{1 - \zeta_I} \\
\xi_{mic} = \delta_p \cdot \eta_{p,w} \\
\dfrac{d\delta_p}{d\vartheta} = C_\delta \cdot \kappa_{p,w}(\tau) \cdot n \cdot {\delta_p}^{-2} \\
\left(1 + \nu_{mic} \cdot [N_{mic}]_{w,0} \cdot \eta_{p,w} \cdot \delta_p^3 + \varepsilon \cdot \vartheta - \varepsilon \cdot \dfrac{d\zeta}{d\vartheta}\right) \cdot \dfrac{d\tau}{d\vartheta} = \Delta\tau_{ad,0} \cdot \left(\dfrac{d\zeta}{d\vartheta}\right) - (Wt \cdot (1 + \varepsilon\vartheta) \cdot (1 - \omega \cdot \zeta) + R_H\varepsilon) \cdot \left(\tau - \tau_{cool}^{eff}\right) \\
-Wt_{ext} \cdot (\tau - \tau_{amb}) - \alpha \cdot [1 + \varsigma \cdot (\tau - \tau_{dos})] \\
I.C \quad \vartheta = 0 \Rightarrow \xi_I = \varsigma_{R,w} = \xi_M = n = \eta_{p,w} = 0 \quad \delta_p = 1 \quad \tau = \tau_0 = \tau_{cool} - 8.33 \times 10^{-3}
\end{cases}
\tag{A.1}
$$

For $\vartheta \geq 1$, all $\varepsilon\vartheta$ terms must be substituted with ε and for $\vartheta \geq 1 + \vartheta_{delay}$, all $[\vartheta/(1 + \vartheta_{delay}) - \zeta]$ must be substituted with $(1 - \zeta)$. The meaning of all terms involved in Eq. (A.1) is reported in the Nomenclature section.

It can be noticed that, in order to analyze the monomer conversion, the chain transfer to monomer reaction has been disregarded because, in the operating temperature range (70–90 °C), the propagation reaction is much faster than it. On the contrary, a monomer dosing delay must be taken into account because VA evaporates during the dosing (boiling point: 72.7 °C) and, then, it is condensed by the means of a total condenser. Finally, a global termination reaction can be considered because the TMK model has been used.

Radical diffusion (inside and outside the micelle/polymer particles), homogeneous (in water) and micelle nucleation with polymer particles coagulation phenomena have also been considered [20].

Moreover, in the energy balance equation, the following heat contributions have been involved: a heat accumulation one (right hand side) responsible for the temperature increase during the process, a heat development one (first term on the left hand side) accounting for the heat developed by all exothermic reactions (in this case, only the propagation reaction), a first heat removal one (second term on the left hand side) due to the combined dosing

stream and cooling jacket action, a second heat removal one (third term on the left hand side) due to ambient heat dispersions and a third heat removal one (fourth term on the left hand side) ascribed to evaporation heat losses.

References

[1] P.F. Nolan, J.A. Barton, Some lessons from thermal-runaway incidents, J. Hazard. Mater. 14 (1987) 233–239.
[2] K.H. Hu, C.S. Kao, Y.S. Duh, Studies on the runaway reaction of ABS polymerization process, J. Hazard. Mater. 159 (2008) 25–34.
[3] J. Brandrup, E.H. Immergut, E.A. Grulke, A. Abe, D.R. Bloch, Polymer Handbook, 4th ed., John Wiley & Sons, Hoboken, 1999.
[4] E. Trommsdorff, H. Köhle, P. Lagally, Zur polymerisation des methacrylsäuremethylesters, Makromol. Chem. 1 (1948) 169–198.
[5] M. Alger, Polymer Science Dictionary, Elsevier Applied Science, New York, 1989.
[6] F. Maestri, R. Rota, Temperature diagrams for preventing decomposition or side reactions in liquid–liquid semibatch reactors, Chem. Eng. Sci. 61 (2006) 3068–3078.
[7] Y.H. Erbil, Vinyl Acetate Emulsion Polymerization and Copolymerization with Acrylic Monomers, CLC Press LLC, Boca Raton, 2000.
[8] S. Copelli, M. Derudi, R. Rota, Topological criteria to safely optimize hazardous chemical processes involving consecutive reactions, Ind. Eng. Chem. Res. 49 (2010) 4583–4593.
[9] S. Copelli, M. Derudi, R. Rota, Topological criterion to safely optimize hazardous chemical processes involving arbitrary kinetic schemes, Ind. Eng. Chem. Res. 50 (2011) 1588–1598.
[10] M. Steensma, K.R. Westerterp, Thermally safe operation of a cooled semibatch reactor. Slow liquid–liquid reactions, Chem. Eng. Sci. 43 (1988) 2125–2132.
[11] F. Maestri, R. Rota, Thermally safe operation of liquid–liquid semibatch reactors. Part I: single kinetically controlled reactions with arbitrary reaction order, Chem. Eng. Sci. 60 (2005) 3309–3322.
[12] F. Maestri, R. Rota, Thermally safe operation of liquid–liquid semibatch reactors. Part II: single diffusion controlled reactions with arbitrary reaction order, Chem. Eng. Sci. 60 (2005) 5590–5602.
[13] F. Maestri, S. Copelli, R. Rota, L. Gigante, A. Lunghi, P. Cardillo, Simple procedure for optimally scaling-up fine chemical processes. I. Practical tools, Ind. Eng. Chem. Res. 48 (2009) 1307–1315.
[14] F. Maestri, S. Copelli, R. Rota, L. Gigante, A. Lunghi, P. Cardillo, Simple procedure for optimal scale-up of fine chemical processes. II. Nitration of 4-chlorobenzotrifluoride, Ind. Eng. Chem. Res. 48 (2009) 1316–1324.
[15] R. Pohorecki, E. Molga, The Westerterp number (Wt), Chem. Eng. Res. Des. 88 (2010) 385–387.
[16] R.H. Perry, D.W. Green, Perry's Chemical Engineer's Handbook, 7th ed., Mc Graw-Hill International Editors, New York, 1998.
[17] ISO Standard 124-1992: Rubber lattices—determination of total solids content.
[18] ISO Standard 976-1986: Rubber lattices—determination of pH.
[19] C. Hagiopol, Copolymerization: Towards a Systematic Approach, Kluwer Academic/Plenum Publishers, New York, 1999.
[20] C. Sayer, M. Palma, R. Giudici, Modeling continuous vinyl acetate emulsion polymerization reactions in a pulsed laser sieve plate column, Ind. Eng. Chem. Res. 41 (2002) 1733–1744.
[21] J.L. Gustin, F. Laganier, Understanding vinyl acetate polymerization accidents, Org. Process Res. Dev. 9 (2005) 962–975.